



# Demonstration of a Precision Missile Intercept Measurement Technique

*Thomas Thompson*

**R**ecently a special Independent Research and Development project demonstrated that translator-based differential Global Positioning System (GPS) measurements can achieve a measurement accuracy of 2 cm in realistic missile intercept test environments. The project was initiated in recognition of a serious need an effective precision analysis capability for use in evaluating engagements and lethality of advanced ballistic missile intercept systems. Without accurate relative trajectory measurements at this level of precision, precision interceptor test and evaluation is impossible; end-point scoring is not sufficient. This article describes the project, which demonstrated that wideband GPS translator instrumentation can provide sub-GPS-wavelength trajectory measurements and offers the most practical approach to providing the required instrumentation.

(Keywords: GPS translators, High-accuracy differential GPS, Lethality testing, Missile test and evaluation, System model validation.)

## INTRODUCTION

The Laboratory has been involved in the design and development of instrumentation for evaluation of precision hit-to-kill weapon systems since the late 1980s. APL participated in test preparation and postflight processing activities for two Ballistic Missile Defense Organization (BMDO) Exoatmospheric Reentry Intercept Subsystem (ERIS) flight tests and developed the instrumentation for the Brilliant Pebbles intercept test program. Although Brilliant Pebbles was canceled before achieving flight test status, APL completed development and flight qualification of the intercept instrumentation system. Both the ERIS and the

Brilliant Pebbles instrumentation systems were based on the use of differential Global Positioning System (GPS) measurements to achieve submeter accuracy. Both used the GPS signal translator concepts pioneered by APL for the Trident Fleet Ballistic Missile (FBM) test and evaluation program. A translator is basically a signal relay device that receives GPS signals, translates them to a different frequency, and then retransmits the translated signals. Translators installed in both the interceptor and target vehicles allowed the differential GPS measurements needed to support precision intercept evaluations. The Brilliant Pebbles

instrumentation required that the interceptor data be encrypted. To meet this translator requirement, APL developed the first missile-qualified GPS digital translator.<sup>1</sup> The target translator for Brilliant Pebbles and the translators for ERIS and the ERIS target used analog technology. Either technique, analog or digital, can be designed to provide the necessary capability, but most of our experience is based on analog translators. In a companion article in this issue, Thompson and Westerfield discuss translators and APL's role in their development.

The ERIS flight test program consisted of two successful flight tests. The first, in January 1991, resulted in a direct hit of the target; the second, in March 1992, resulted in a near miss. The differential GPS measurements of the relative position vector (i.e., the vector formed by joining the tip of the interceptor to the aim point on the target) were recorded throughout the encounter. In both tests, the relative position vector uncertainties, measured at a 10-Hz rate, were less than 60 cm. In the first test, the final GPS vector measurement point determined after the flight confirmed the observed direct target impact. In 1993, we completed a brief study to determine if the ERIS measurement technique was capable of providing the same relative position measurement with an uncertainty of less than 2 cm. The study concluded that 2-cm measurements were possible with modifications of the ERIS translator system, but none of the required equipment was available. Recognizing a real need for a new kind of GPS translator, we initiated an Independent Research and Development (IR&D) project to demonstrate a low-cost design approach for the required translator.

In a totally unrelated series of events, a need for this same type of translator arose in the Extended Navy Test Bed (ENTB) system. The ENTB is a test reentry body system needed to support special Trident FBM reentry body tests. On the basis of this need, APL undertook a quick-response development program, founded on concepts developed from the IR&D effort, to develop a new GPS translator system for the ENTB. APL developed both the improved translator and the special portable ground station receiving/recording equipment needed to support Trident reentry body testing. After successful completion of the first ENTB flight test in December 1995,<sup>2</sup> the Navy allowed APL to use equipment available from the ENTB development activity for a new IR&D project to demonstrate the capability for a 2-cm relative position vector measurement that was defined in our 1993 study. That IR&D project is the subject of this article, which draws technical information from three earlier papers.<sup>3-5</sup>

## WHY 2 CENTIMETERS?

Why are 2-cm vector measurements of the relative trajectory between an interceptor and target needed?

Even accepting that the lethality requirement for hit-to-kill weapons might result in accuracy requirements measured in small numbers of centimeters, isn't it sufficient to provide a measurement of the hit point to within 2 cm? Or, if a measurement of the impact's result (for example, radar debris cloud analysis) can provide a sure indication of a lethal hit, isn't that sufficient? The answer to both questions is no! Unless the component contributors to system inaccuracy are very much smaller than the total system requirement, end-point scoring will not provide the understanding required for confident predictions of actual system performance in a tactical environment. The situation for precision interceptor weapon systems now is analogous to the situation that existed for the Trident FBM when the Improved Accuracy Program was initiated. In both situations, the required accuracy is on the same order as the system's projected capability. In such cases, a number of component and/or subsystem errors are significant relative to the accuracy requirement, and the underlying system models must be well understood for confident assessment of kill probability. In this circumstance, attempting to confidently determine kill probability by seeing if end-point scoring results are consistent with simulations can lead, at best, to an excessive number of flight tests; at worst, it can give invalid results. If the system model indicates that test results are a function of various trajectory and/or environmental characteristics, the scoring results will either absorb those effects, or the flight test program will need to expand to gather statistics for representative samples of trajectory and environmental conditions. In no case does the impact scoring approach provide insight into the adequacy or representativeness of the underlying weapon system error models.

The engineering development community must produce an integrated system performance model to develop a system that can meet its performance requirements. For the system being developed, of course, such a model includes no flight test experience. In many instances, a substantial base of previous experience is available for initial estimates. However, in the domain of ballistic intercepts, virtually no comparable system test experience supports *a priori* models. The integrated system model is derived from individual subsystem models, with which we have a wide range of application experience, and many of the subsystem models are confirmed by testing in a variety of environments. However, experience with subsystem models does not assure that these models will be valid in the actual flight environments to be experienced in the system being developed. Connecting the outcome of model simulations with the flight test scoring results can provide no insight with regard to model errors representing the actual flight test environments. Such validation, with attendant confidence statements, requires a measurement of flight test

performance that can provide observations of terms of fundamental underlying model error components. It requires trajectory measurement data with sufficient continuity and precision to allow observation of the underlying guidance and control functions, including the seeker, within the flight test environment. The Trident test and evaluation experience, and even the Laboratory's limited U.S. Air Force Peacekeeper test and evaluation experience, have amply demonstrated the correctness of this conclusion. The clear need for flight test performance measurements for use in model validation motivated the IR&D project discussed in this article. Only end-game relative trajectory measurements that provide nearly continuous observation of motion dynamics to a fraction of the intercept accuracy requirement, under representative flight conditions, can validate the underlying guidance and control models of the system. To assure successful deployment of precision ballistic intercept systems, an instrumentation system with 2-cm precision must be an integral part of any comprehensive test and evaluation program.

## THE TEST CONFIGURATION

The concept demonstration was conducted at the Holloman Air Force Base's High-Speed Test Track on 9 August 1996. The test included two GPS translator-equipped instrumented test bodies, one rocket propelled on one rail of the test track and the other stationary on the second rail. The dynamic sled consisted

of one instrumented body attached to a 23-cm (9-in.) diameter rocket (the second stage) and a pusher using a stack of seven smaller rockets (the first stage), as shown in Fig. 1. Both instrumented bodies had the same type of GPS antenna, which was designed specifically for conformal mounting on the test bodies. The dynamic body used an S-band blade antenna to relay the translated GPS signals to the antenna at the Track Data Center. A second blade antenna transmitted the body telemetry signals. A cable carried S-band signals from the stationary body to a track-side blockhouse. Translated GPS signals were recorded at both sites using ENTB receiver and recording equipment. A closer view of the two instrumented bodies is shown in Fig. 2. This photograph was taken during a slow run-through test conducted one day before the actual rocket test. The dynamic body is in the foreground. The large equipment behind the stationary body is a portable air conditioning unit that supported the long preflight test activities. It was removed before the rocket test.

The track is equipped with a location measurement system, known as "Spots," based on magnetic interrupters. Time of day is recorded as the sled passes each interrupter. The accuracy of this system is limited by uncertainties in the exact position and timing of the interrupter. Higher-precision positioning was provided by additional track instrumentation in the region of closest approach between the dynamic and stationary bodies. An image motion compensation camera photographed the dynamic sled at the point of closest

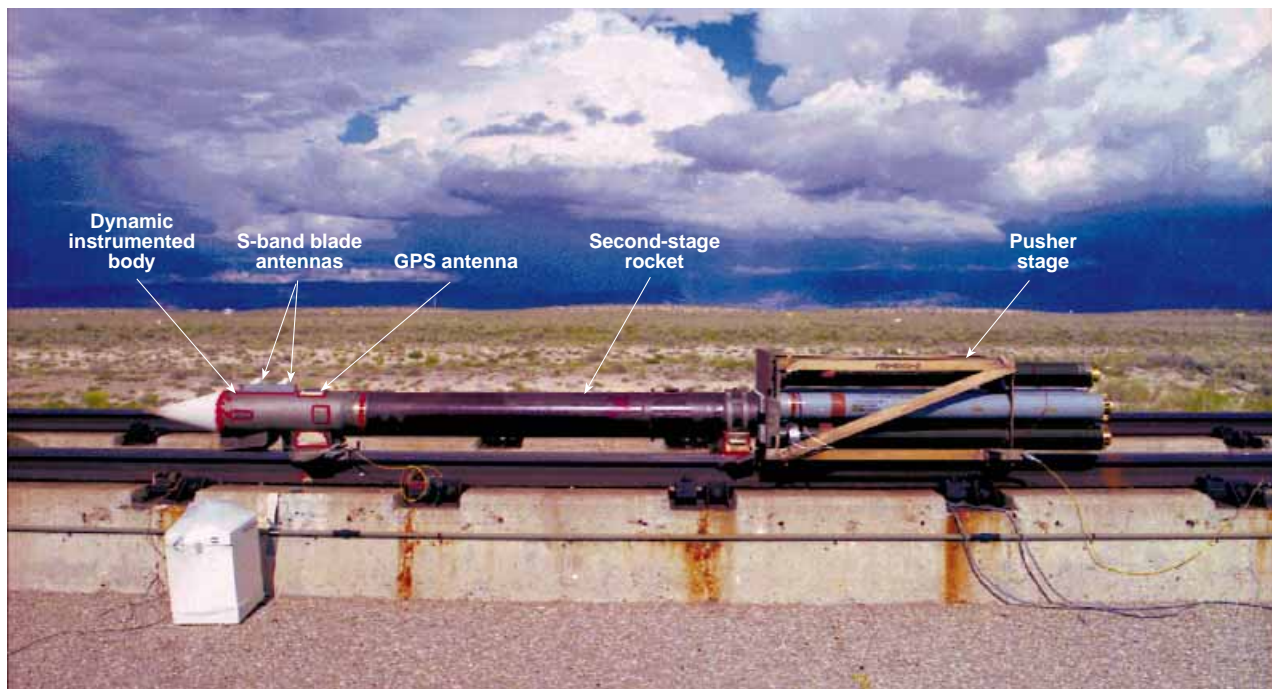


**Figure 1.** Dynamic sled at launch point. The instrumented body is directly behind the nose cone, with two S-band blade antennas on top and the GPS antenna directly behind them. The second-stage rocket has a 23-cm (9-in.) diameter and is about 2 m (7 ft) long. The first stage (or pusher) consists of a stack of seven smaller rockets.



**Figure 2.** Instrumented bodies during checkout. The dynamic body has S-band and GPS antennas mounted on top; the stationary body has only a GPS antenna. Both bodies have GPS signal translators mounted inside, and the dynamic body also includes internal telemetry functions. Telemetry and translator signals are communicated through the two S-band antennas on the dynamic body. An RF cable carries S-band signals from the stationary body to a track-side block house. The air conditioning unit in the background (used during checkout) was removed before the sled test.

approach. This photograph was analyzed to measure displacement of the dynamic GPS antenna relative to its rest position (i.e., the condition where precision survey measurements were taken). In addition, a precision fiber-optic system was used to accurately measure the time of closest approach and the time at three positions on either side of the closest approach point. Together these systems provided an independent measurement, to a fraction of a centimeter, of the relative position vector in the region of closest approach. This instrumentation was provided by the Holloman facility. Holloman track staff operated it and analyzed the results. APL used the track measurements as ground truth for evaluating GPS measurements derived from translator processing.

## TEST DYNAMICS

The need to provide a high-speed intercept-like test condition with an accurate, independently measured trajectory led to selection of the Holloman facility. The dynamic conditions as measured by an onboard accelerometer are shown in Fig. 3. In many ways the test track environment is more stressful than most (maybe all) real missile intercepts. In our test, the dynamic sled accelerated to a speed of 5000 km/h (3100 mi/h) in less than 1.6 km (1 mi) of travel. Being held captive to the track with high acceleration produced rather large vibration accelerations in all directions. Finally, each ignition and cutoff event created jerk levels of  $-300$  to  $1500$  times the force of gravity per second ( $G/s$ ) (jerk is measured as the rate of change in acceleration). To

exercise the GPS tracking system at or near the highest velocity point, one of the higher-jerk conditions was created at the point of closest approach. The ability to maintain continuous-phase tracking of the GPS signals through these very demanding conditions is a prime reason for recommending translators (rather than GPS receivers) for highly accurate intercept instrumentation. With translators, all phase tracking is done after the flight through playback of recorded signal data, which allows the process to be repeated for as many iterations as necessary. GPS signal translation, broadband signal sampling, and recording are very much simpler and more robust processes than those required for real-time GPS receivers. Recognizing the substantial investment associated with missile intercept testing, it makes good economical sense to use translators for this purpose.

Figure 4 shows the basic geometry and defines the coordinate system for our measurements. Relative position vector measurements are defined in terms of three

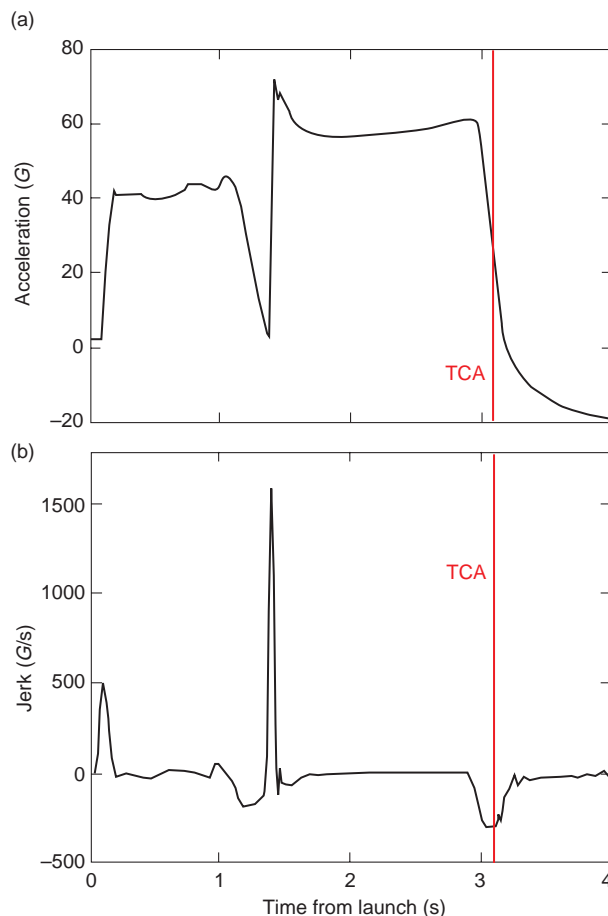


**Figure 3.** Sled dynamics. (a) Sled acceleration profile during the first 4 s of the test. The first-stage pusher achieves a 40-G thrust level, and the second stage sustains about a 60-G thrust level. At time of closest approach (TCA), the sled was near maximum velocity (5000 km/h, or 3100 mi/h). (b) Jerk levels experienced over the interval. The most accurate measurements are required near TCA, where the jerk is at a sustained level of approximately  $-300$   $G/s$ .

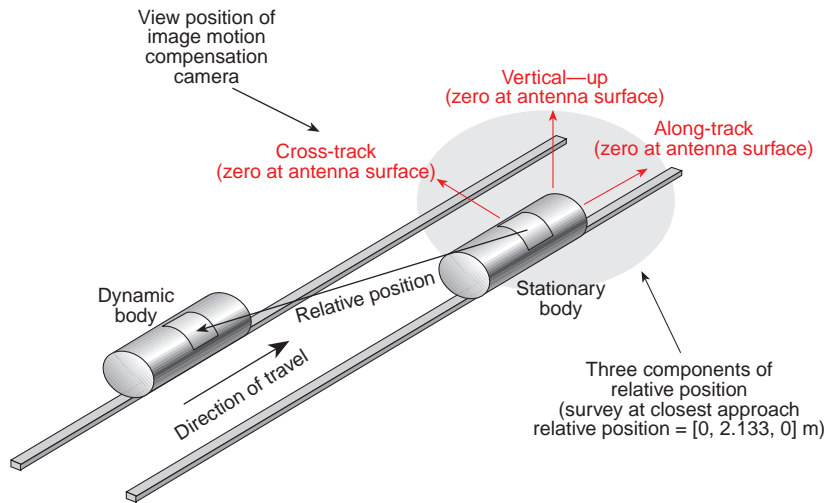


**Figure 4.** Test geometry. The origin is at the center of the GPS antenna on the stationary body. During the dynamic flight, the relative position vector was accurately measured in relation to the vector components shown. The image motion compensation camera was used for optical measurements; additional optical measurements were made with fiber-optic break cables (not shown) located at closest approach and at three evenly spaced locations on either side of closest approach.

orthogonal components: along-track, cross-track, vertical. The origin is at the center of the stationary body's GPS antenna. The along-track direction is aligned to the nominal direction of the track and set to be parallel with the local tangent at the stationary body track location, with positive defined as the direction of travel. Vertical is positive up, and the cross-track direction is positive toward the other rail. The surveyed relative position vector at closest approach is (0, 2.133, 0) m.

## GPS SIGNAL PROCESSING

GPS positioning with subwavelength accuracy (i.e., <19 cm) depends on a process that determines distances based on carrier-phase measurements. Carrier-phase measurements are produced by a phase-locked signal tracking process. The signal tracker continually tests the phase of a locally generated signal with the received carrier frequency and provides a feedback process that forces the local signal to be phase-matched with the received carrier to a small fraction of a cycle. Phase of the tracked signal is a direct measure of distance to the signal source to a fraction of a wavelength, but it is ambiguous with regard to the total number of wavelengths. Range code modulations associated with the GPS signals provide an unambiguous measure of total distance, but they can't provide subwavelength measurement accuracy of the carrier signal. Normally carrier-phase measurements are used to determine changes in distance over specific tracking intervals (i.e., integrated Doppler). Absolute positioning based on carrier-phase measurements is precluded by errors in satellite position, satellite clocks, and signal propagation, all of which are

large relative to subwavelength precision. However, GPS measurements can be used for relative positioning between two bodies with this technique. Satellite position and clock errors are highly correlated whenever the distance between the two bodies is small relative to the scale of the satellite distances. This condition can be achieved over quite wide separations. Propagation errors usually limit the applicable separation before the satellite errors limit it, and in most cases tropospheric errors set the limit somewhere in the region of 10 km. In any event, this type of measurement is ideally suited to missile intercepts, since the distance between bodies is approaching zero in the region of interest.

In our study the relative position is calculated on the basis of double differences formed by computing the body-to-body difference of common satellite-to-satellite differences for each body. The satellite-to-satellite difference removes all hardware error contributions beyond the body's GPS antenna, and the second difference removes the systematic propagation and satellite errors. The primary errors in the second difference are due to thermal noise in the signal tracking loops. The postflight tracking system actually tracks each translated satellite signal individually. The process is aided by taking advantage of the along-track accelerometer measurements and a "pilot carrier" tracking process (the pilot carrier is a signal produced in the translator as a direct multiple of its oscillator frequency). Without these aids it would be extremely difficult, perhaps impossible, to track the translated GPS signals. The process is iterative; aids for successive tracks are improved using the results of previous tracks. When the tracking process was completed, the tracking data for the six available satellites were used to produce the double-difference data required to compute the relative position vector.

Although the final measurement precision is based on carrier-phase measurements, the ranging noise can't be ignored. Its importance can be understood in relation to the signal processing technique needed when GPS carrier-phase techniques for distance measurement are applied to dynamic situations. The techniques known as "wide-laning" and "narrow-laning" use tracking data from both GPS signal frequencies (designated  $L_1 = 1575.42$  MHz and  $L_2 = 1227.6$  MHz) to help define the ambiguity integers. Differences of the measured data at the two GPS frequencies produce a computational wavelength that is larger than either signal's

wavelength, and the sum produces a smaller computational wavelength. Wide-lane phase and narrow-lane range are computed as

$$\Phi_{\Delta} = \Phi_1 - \Phi_2, \quad (1)$$

$$R_{\Sigma} = [(R_1/\lambda_1) + (R_2/\lambda_2)] \lambda_{\Sigma}, \quad (2)$$

where  $\Phi_1$ ,  $\Phi_2$  and  $R_1$ ,  $R_2$  are the double-differenced phase and range measurements at  $L_1$  and  $L_2$ ; the subscripts  $\Delta$  and  $\Sigma$  refer to wide lane and narrow lane, respectively; and  $\lambda$  is the wavelength at the frequency indicated by its subscript. Real-valued estimates of the wide-lane and the narrow-lane integers can be computed as follows:

$$N_{\Delta}(\text{real est.}) = \Phi_{\Delta} - R_{\Sigma}/\lambda_{\Delta}, \quad (3)$$

$$N_{\Sigma}(\text{real est.}) = (1 - k_1) \Phi_1 + (1 + k_1) \Phi_2 + k_1 N_{\Delta} + k_2 (\text{ionosphere @ } L_1), \quad (4)$$

where the constants  $k_1$  and  $k_2$  are defined by

$$k_1 = \lambda_{\Delta} / \lambda_{\Sigma} = 8.059,$$

$$k_2 = 2(1 + \alpha) / \lambda_1,$$

using the wavelength ratio  $\alpha = \lambda_2 / \lambda_1$ .

Errors in ionosphere, troposphere, and timing vanish in the wide-lane integer computation. Because range noise is large, however, smoothing is normally applied over an appropriate data span to provide a mean value that can then be rounded to the nearest integer. For the narrow-lane integer estimate, tropospheric and timing errors vanish, and the ionospheric error is often assumed to be zero. The estimate contains only phase data explicitly, although an integer wide-lane value (previously fixed using the range and phase data) is needed in the computation. The  $L_1$  and  $L_2$  integers are then obtained as

$$N_1 = (N_{\Sigma} + N_{\Delta}) / 2, \quad (5)$$

$$N_2 = (N_{\Sigma} - N_{\Delta}) / 2. \quad (6)$$

Since  $N_1$  and  $N_2$  must be integers,  $N_{\Delta}$  and  $N_{\Sigma}$  must either both be even or both be odd. If this condition is not met, then  $N_{\Delta}$  and  $N_{\Sigma}$  are adjusted to the most likely pair of integers.

A reference trajectory for the dynamic body relative to the stationary body was obtained by taking advantage of 60 s of tracking data prior to the rocket launch. These data were used to compute the ambiguity integers at the launch time, taking advantage of the fact that both bodies were stationary and the relative propagation errors were insignificant (i.e., the bodies were separated by less than 2 km). Using these data, the narrow-lane integer ( $N_{\Sigma}$ ) tracks were formed for the 20-s flight time. The resulting tracks for each double difference are shown separately in Fig. 5. The satellite differences are indicated by their pseudorandom noise (PRN) numbers. (PRN numbers define the range code assignments for each satellite, and satellites are commonly designated by this number.)

The six satellites tracked provide five independent tracking differences shown using PRN14 as the common satellite. The data in Fig. 5 are shown at the 10-Hz rate, and each data point depends on data from eight phase-locked loops (i.e., two satellites and two frequencies for each body). The double-difference data are integrated continually from the initial time point to the end of the flight. In two of the plots there is no break in the narrow-lane integer (i.e., cycle count), indicating that continuous phase tracking was achieved for these data throughout the 20-s flight. The other plots show distinct steps in the integrated double-difference phase data. Each step results from a momentary loss of lock, which produces a discontinuity in the wavelength (i.e., cycle) count. In the particular tracking configuration used for this test, cycle jumps could occur in integer numbers of half cycles. Because the narrow-lane integer includes the wavelength multiplier  $k_1$  (see Eq. 4), half-cycle slips result in minimum step sizes of about 4.5 cycles in the narrow-lane cycle count. Since the quality of the tracking data was so good, these data could be used to accurately correct for the discrete jumps. Once corrected, all narrow-lane integer data matched the quality of the two continuous tracks. Corrections were then applied to the data for accurate clock histories for each recording site (estimated from the GPS data to less than 100 ns), full nonlinear geometry, and propagation times for all signal links, as well as separate tropospheric corrections (accounting for geometric differences, but using a common symmetric tropospheric model). Corrected phase measurements were then produced for wide-lane,  $L_1$ , and  $L_2$  data. These data were then used to produce a best estimate of trajectory for the dynamic body relative to the stationary body.

The quality of the final corrected tracking data was tested by examining the difference between the theoretical double-difference data (using the final best estimate of trajectory and the satellite ephemeris information) and the corrected measurement data (i.e., the

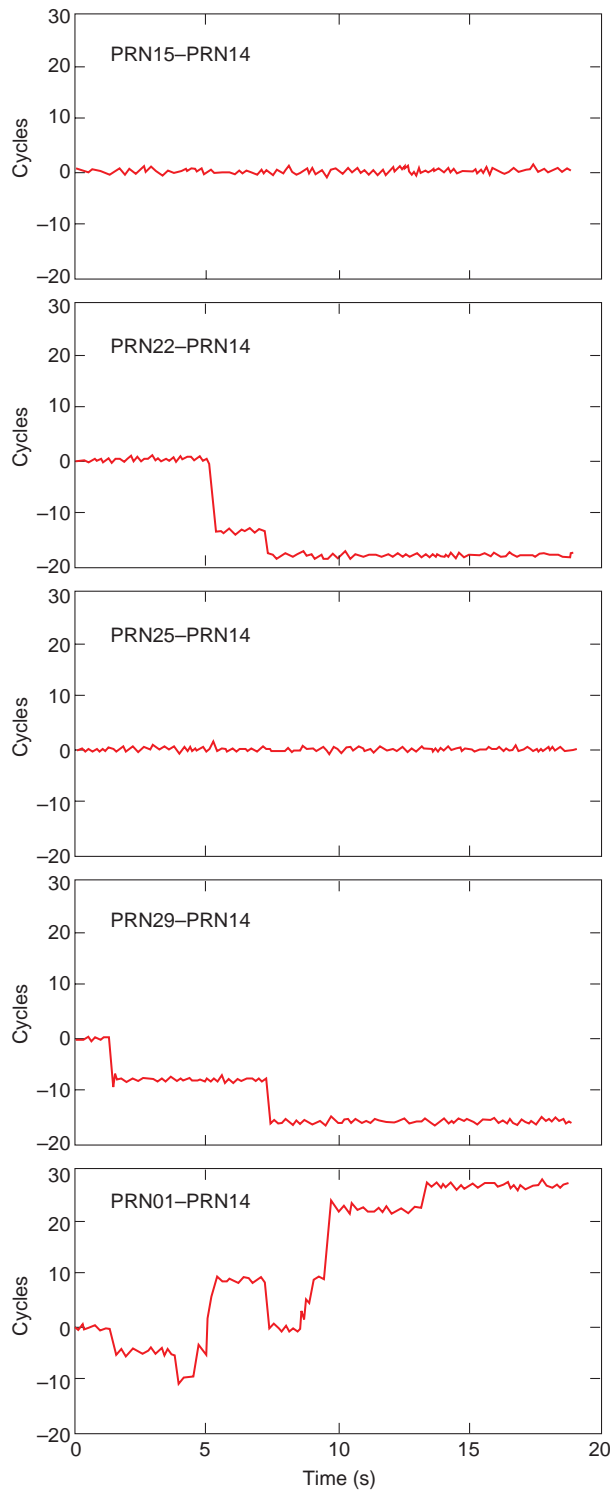


**Figure 5.** Narrow-lane integers (cycles) before correction for cycle slips: the wavelength integers for the sum of the two GPS frequencies as they varied during the 20-s ride (referenced to the values computed for the 60-s period before launch). Measurements for five independent satellite differences are plotted, identified by each satellite's pseudorandom noise (PRN) code number. Momentary cycle slips in the phase-locked tracking loops caused jumps in the integer values having precise quantification levels that were subsequently computed and corrected. Each data point (at 10 samples/s) contains data from eight 10-Hz phase-locked loops (two satellites, two frequencies, two bodies).

tracking residuals). Figure 6 shows the residuals for the  $L_1$  tracking data. The tracking residuals clearly demonstrate that the correction and ambiguity algorithms worked perfectly. The mean of the five satellite  $L_1$  double-difference residuals used by the estimator was 0.1 cm, and the variance was 0.6 cm. The largest residual data point was less than 3 cm in the complete data set (i.e., less than 0.16 wavelengths). The  $L_2$  data showed similar results, with a total mean of 0.4 cm and a variance of 0.8 cm. This process proves that the internal consistency of the data is good to well within a wavelength. Accuracy is demonstrated in a later section of this article by a comparison between the GPS measurements and the optical measurements. However, we first consider how the GPS measurement would be made if the prelaunch initialization process were not available.

## SHORT-SPAN PROCESSING

The circumstances of the sled test allowed the luxury of initializing the relative positioning process from a stationary condition, which would be impossible in many missile intercept scenarios. A second processing methodology was tested to demonstrate that the same measurement precision could be achieved with only short spans of dynamic data. Three separate data spans were selected; in each, neither GPS data outside that span nor onboard acceleration data were used in any way to initialize or aid the process. The data rate was 10 Hz for all three cases. The time spans analyzed were (a) 1.2 s, ending at the point of closest approach (to simulate an intercept condition); (b) a very short span of 0.6 s centered on closest approach (a miss condition); and (c) a 3-s interval when the bodies were more widely separated (a “big miss” condition—8 km in this case). The difficult dynamics near closest approach are shown in Fig. 3. In case (c), data near the end of the flight were used to include the two separate sled water brakes that produced step changes in acceleration of 5–10 G.

For each case, the processing proceeded as follows. A standard algorithm was used to provide initial guesses of the wide-lane and narrow-lane integers. This algorithm was the same as that described for the longer-span GPS signal processing (Eqs. 1–4). Concurrently with this integer initialization process, the narrow-lane techniques described earlier were used to detect and correct as required any cycle slips that may have occurred during the short data intervals (see Fig. 5). Initial values for  $L_1$  and  $L_2$  were then obtained from the wide-lane and narrow-lane initial guesses. These initial values were expected to be poor because the initial wide-lane (and hence narrow-lane) estimates depend on range data, and the short data spans afforded very limited range smoothing. Full corrections were then applied to the phase data, using a reference trajectory approach (based on only the

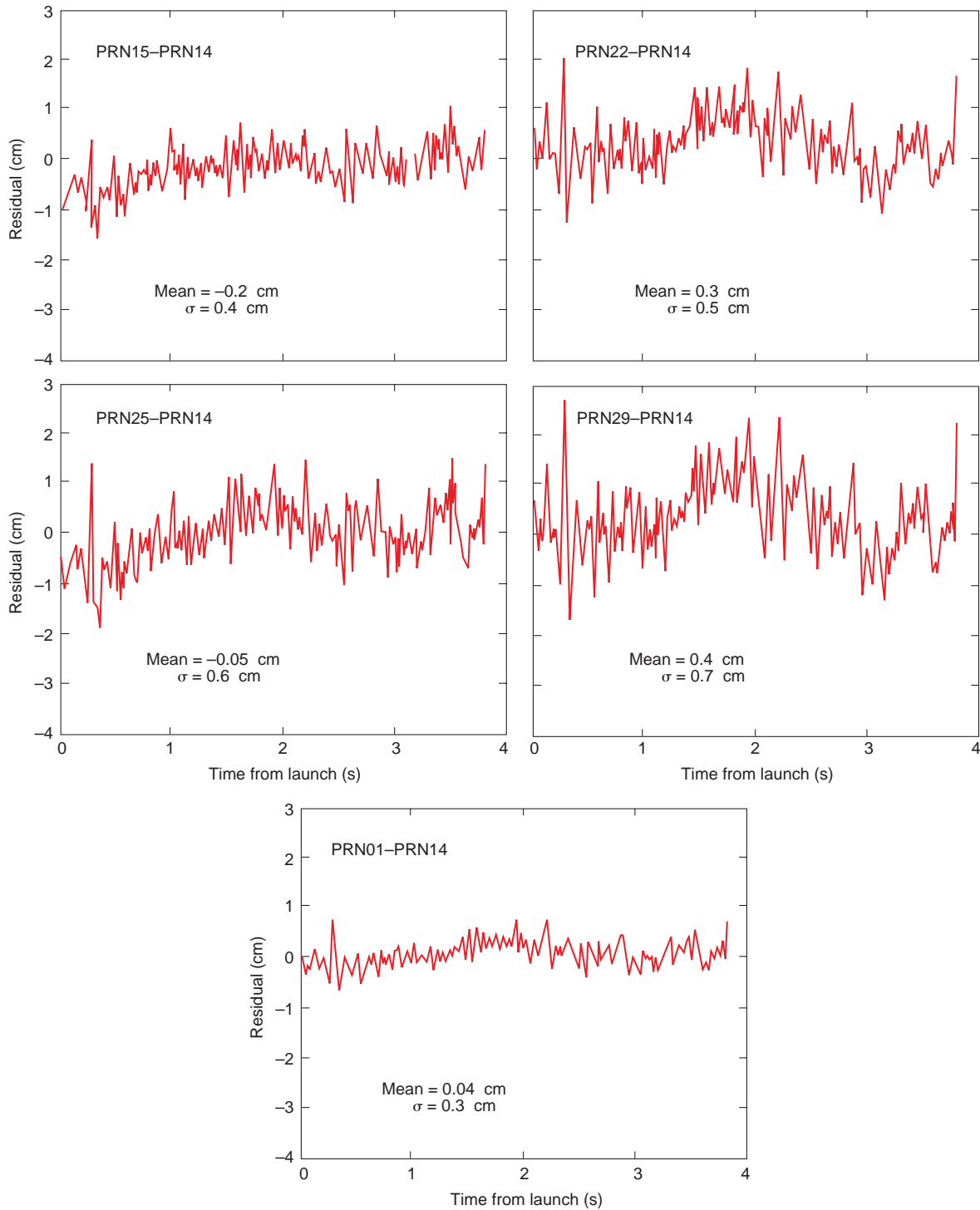


**Figure 6.**  $L_1$  measurement residuals. Each plot shows the difference between the theoretical values (based on the GPS-derived dynamic body trajectory and GPS ephemeris estimates) and the measurement data after the wide/narrow-lane correction process. All residuals fit easily within the  $-4$  to  $+3$  cm axis shown, which is very much less than the 19-cm wavelength of the  $L_1$  signal. (For all data, mean = 0.1 cm,  $\sigma = 0.6$  cm.) The data clearly demonstrate the quality and continuity of track realized by the measurement process.

data in the selected interval), as previously described for longer-span GPS signal processing.

The next step was to perform an exhaustive search to find the set of integers that minimized a scalar figure of merit (FOM) as follows. For a given integer set, the

corresponding measurements are used in a least-squares procedure to estimate the relative position vector. The FOM is the quadratic form of the resulting residuals weighted by their inverse covariance matrix. The search is performed by sequentially incrementing each



double-differenced measurement through integer values from the initial value out to a distance corresponding to the  $3\text{-}\sigma$  uncertainty in the initial integer guesses. Statistically, the lowest value of the FOM corresponds to the correct integer set. Taking advantage of the two independent frequency measurements, the resulting search achieved a minimum FOM value for all three cases when the short-span ambiguity integers matched the values achieved in the reference trajectory process. Therefore, the relative position vector over each span achieved the same precision as that provided by the reference trajectory.

The short-span processing test clearly demonstrates that a robust ambiguity resolution is possible with very short spans of high-quality differential GPS tracking data. The cases considered here are surely extreme. Even in cases where a stationary starting condition is impractical, there will surely be “quiet” trajectory regions where good-quality initialization is possible. In fact, it would be foolish to not take advantage of the translator capabilities over as much of the flight regime as possible. Full trajectory measurements will provide deeper insights into interceptor performance, and if the ground station is properly configured, the translator signals can be used to perform the range safety function for the interceptor and target vehicles.

## SYSTEM ACCURACY

The full- and short-span signal processing results provide clear evidence that the measurement process can readily support very accurate relative positioning in an intercept environment, but the final proof requires comparison with the independent measurements provided by the Holloman test track analysts using data from the independent optical instrumentation.

The GPS cross-track relative position measurement (with surveyed rail separation removed) is shown in Fig. 7 for  $L_1$  and  $L_2$  frequencies. A true error can be estimated only near the point of closest approach, where the survey measurements were made. However, if the rails were perfectly straight and our coordinate frame perfectly aligned with the track, the cross-track component of the relative position vector would be constant (i.e., equal to the survey measurement at closest approach—represented as zero in the figure). If these measurements had a single slope, a slight rotation of our coordinate system could remove it, but the data span contains a break point. We could select an orientation that minimized the deviation, but the most significant point to be made regarding these data is that we are looking at a few centimeters’ variation over a track span of more than 10,000 m!

The GPS measurement of relative cross-track position in the survey region is shown in Fig. 8a. The GPS measurement in this figure is based on combining data

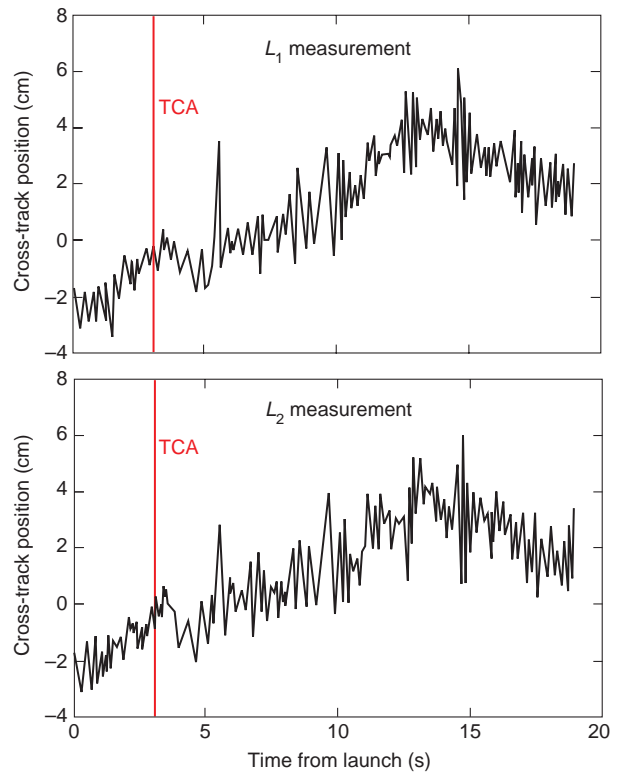


**Figure 7.** Cross-track errors. The two plots ( $L_1$  and  $L_2$  measurements) indicate the apparent cross-track error (based on an assumed constant track separation and direction). Both frequencies indicate the same structure. If a single slope change would correct the error, it could be made with a small rotation of the reference coordinate system. Independent measurements of the required accuracy are available only in the region of the time of closest approach (TCA), but it is interesting to note that the apparent errors are only a few centimeters over the full 10-km run.

from both frequencies. If we assume the survey data are perfect, the GPS measurement error in the cross-track direction would be  $-0.3$  cm with an uncertainty of 0.6 cm. (The error value is based on the mean difference for the five GPS points nearest the time of closest approach.) Similarly, the vertical component of the relative position vector in the region of closest approach is shown in Fig. 8b. Determination of along-track difference is based on a comparison of the GPS relative along-track position, with the fiber-optic break cable measurements made with the seven fiber-optic positions centered on closest approach. Figure 8c shows that comparison.

The difference in the observed relative position vector components between the survey measurements and the GPS measurements is summarized in Table 1. The survey measurements, combined with fiber-optic and camera processing uncertainties, are assessed to produce an error of less than 1 cm in the reference position used for comparison with the GPS data. The differences given are the GPS measurement minus the optical survey measurement for the three components

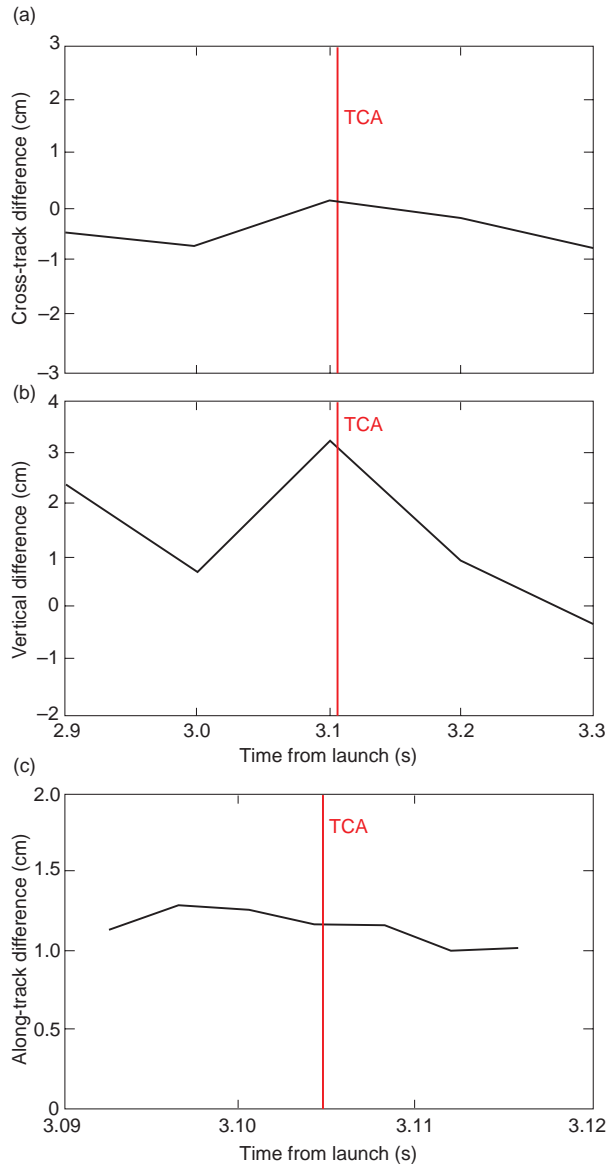


**Figure 8.** Comparison of GPS relative position measurements with the independent optical survey. (a) Cross-track errors near time of closest approach (TCA) show a mean difference for the five points of  $-0.3$  cm. (b) Vertical errors near TCA show a mean difference for the five points of  $+1.4$  cm. (c) Along-track errors near TCA show a mean difference for the seven points of  $1.1$  cm. The time axis is much shorter for the along-track data because of the position of the fiber-optic break cables.

of the relative position vector. The uncertainties shown are those associated with the GPS measurement process determined by the total GPS estimation process. A detailed statistical characterization of the optical measurement system was not provided; it was specified only as being accurate to less than 1 cm. The differences can be considered relative position errors only if the surveyed data are assumed to be errorless. In any event, the differences between the reference and the GPS

**Table 1.** Measurement differences between the GPS-derived values and the precision optical survey values for each coordinate of the relative position vector at the point of closest approach. The optical survey precision was characterized as being accurate to less than 1 cm.

Component	Difference between GPS and optical values (cm)	Uncertainty in GPS estimate (cm)
Along-track	1.1	0.8
Cross-track	-0.3	0.6
Vertical	1.4	1.8

measurements are shown to be less than 2 cm in all coordinates, with the maximum difference in the vertical measurement. The data clearly verify that a translator-based GPS relative measurement system can provide 2-cm accuracy in a highly dynamic environment.

## CONCLUSION

We have long been convinced, on the basis of analysis and substantial experience with GPS translator-based precision missile tracking, that this technique could achieve 2-cm measurement precision in a missile intercept flight test environment. Now a test at Holloman's High-Speed Test Track has clearly demonstrated that capability for the first time. The virtues of GPS measurements for this application are compelling. In addition to intercept and lethality evaluations, this single-instrumentation concept can provide interceptor guidance evaluation capability (which can and should be used to further refine the impact/miss measurement), as it has for Trident since 1978, and range safety tracking support, as it has for Trident since 1987. We know of no other system that can provide all these capabilities. Furthermore, GPS is truly global; it will provide these capabilities at all test ranges.

## REFERENCES

- Devereux, W. S., Duven, D. J., and Boehme, M. H., "The GPS/Telemetry Transmitter (GTT)—A Small GPS Transdigitizer and Telemetry Transmitter," AIAA Paper 93-2693, in *Second Annual AIAA Interceptor Technol. Conf.*, Albuquerque, NM, pp. 1-9 (1993).
- Hattox, T. M., Kinnally, J. J., Mochtak, S. J., and Farrell, W. J., "Postflight Performance of GPS/INS Navigation for a Hypersonic Reentry Body," in *Proc. AIAA Missile Sci. Conf.*, Monterey, CA, pp. 570-578 (Dec 1996).
- Thompson, T., Levy, L. J., Dougherty, J. M., and Hattox, T. M., "Two-Centimeter Measurement System for Missile Intercept T&E," in *Proc. AIAA Missile Sci. Conf.*, Monterey, CA, pp. 189-198 (Dec 1996).
- Thompson, T., Dougherty, J. M., and Hattox, T. M., "Application of GPS to Two-Centimeter Test Missile Intercept Measurements," in *53rd Annual Institute Navigation Conf. Proc.*, pp. 119-130 (Jun-Jul 1997).
- Thompson, T., Devereux, W. S., and Dougherty, J. M., "An Instrumentation System for Lethality Evaluation of Missile Intercept Flight Tests," in *Proc. Sixth Annual AIAA/BMDO Technol. Readiness Conf.* (Aug 1997).

ACKNOWLEDGMENTS: I am grateful for the support and cooperation of the Navy's Strategic Systems Programs organization. Their leadership throughout, and the specific impetus provided by the Extended Navy Test Bed Program, provided the foundation for this work. I particularly thank Marc Meserole for his encouragement. Thanks are also due for

the special work of the APL test and analysis team: Steven F. Bergmann, James R. Brown, James M. Dougherty, Michael M. Feen, Thomas A. French, Thomas M. Hattox, Sung H. Lim, and Glenn T. Moore. Finally, I would like to thank the Holloman High-Speed Test Track team for their excellent support.

## THE AUTHOR



THOMAS THOMPSON received a B.S.E.E. from Lafayette College in 1960 and an M.S.E.E. from The Johns Hopkins University in 1968. He is a member of the Principal Professional Staff in the Strategic Systems Department. He joined APL's Space Department in 1960 and served as a Group Supervisor, a Branch Supervisor, and the Chief Engineer. He participated in a wide range of satellite development activities before becoming the lead system engineer for SATRACK development in 1973. In 1983, Mr. Thompson joined System Planning Corporation, where he led the development of specialized radar instrumentation. Since returning to APL in 1992, he has led the development of important upgrades to the SATRACK system for Trident reentry body flight test evaluations and IR&D activities to demonstrate new GPS measurement capability for missile intercept evaluations. His e-mail address is [thomas.thompson@jhuapl.edu](mailto:thomas.thompson@jhuapl.edu).